Macroscopic-Oriented Gold Nanorods in Polyvinyl Alcohol Films for Polarization-Dependent Multicolor Displays

Liwei Dai, Xuefei Lu, Liping Song, Youju Huang,* Baoqing Liu, Lei Zhang, Jiawei Zhang, Si Wu,* and Tao Chen*

Due to their abundant optical colors, durable color generation, and high refreshing rate, smart chromic nanomaterials (SCNMs) have been employed in various applications. However, most SCNMs often require multicomponent materials, precise morphology control, and complicated modulation to realize multicolor changes, which limits their widely practical applications. In the present study, a simple and effective strategy is demonstrated to achieve the flexible and cost-effective multicolor gold nanorods (Au NRs)/polymer hybrid film, by tuning macroscopic-oriented Au NRs in films and a synergy of polarization-dependent surface plasmon resonance. Au NRs are first functionalized with methoxypoly(ethylene glycol)thiol to improve the compatibility, ensuring Au NRs can be homogenously dispersed in the polyvinyl alcohol (PVA) matrix with high particle density. The macroscopic-oriented alignment of Au NRs can be achieved by the elongation of the PVA polymer molecular chains. Under different polarized excitation directions, the same strip of the hybrid film exhibits various colors including red, orange, yellow, and green. Therefore, the strategy provides a simple and powerful approach to achieve macroscopic-oriented anisotropic nanoparticles in the polymer matrix, and the resultant hybrid films are promising in various practical applications, such as color displays, optical devices, and plasmonic biosensors.

1. Introduction

Smart chromic nanomaterials (SCNMs) have received significant attention in recent years because of great promise for a wide range of applications including biomimetic camouflage,[1,2] optical patterning,[3,4] optical data storage,[5,6] display devices,[7,8] electrochromic devices,[9,10] colorimetric sensors,[11,12] and so forth. At present, there are various building blocks to construct the SCNMs, such as photonic crystals, semiconductor nanoparticles, fluorescent molecules, and partial organic photoresponse molecules and their colors are alterable through Bragg diffraction,[13,14] photoluminescence,[15,16] electrochromism,[17,18] and other stimulating means. To date, much effort has been devoted to the fabrication of the SCNMs. Kim and co-workers[19] reported a facile and practical method for the fabrication of highly transparent colloidal photonic crystal films that can show multiple colors through the overlapping of distinct layers. Rogach and co-workers[20] developed an optical approach to highly align emissive CdSe/CdS core–shell semiconductor nanorods (NRs) and the ordered area can display the color change. Zhu and co-workers[21] reported the design of multicolor fluorescent polymers that shown a color palette from blue to orange under similar excitation conditions. Although these SCNMs can exhibit a variety of colors, it still remains a big challenge to obtain richer colors in a wide spectrum, which impedes their potential applications like full-color electronic paper and electronic device screens.

Noble metal nanoparticles are well known for their unique optical properties arising from the surface plasmon resonance (SPR). They usually generate abundant plasmonic colors by precisely modulating the SPR that highly depends on their sizes, morphologies, compositions, and dielectric environment.[22–25] Compared to other optical colors, the plasmonic color has distinctive optical performance including high color contrast, high resolution, and everlasting colors.[26] More importantly, full colors covering the whole range of the visible light can be obtained by selecting suitable plasmonic materials and nanostructure. For example, Chu and co-workers[2] reported reversible full-color plasmonic cell/display by electrochemically controlling the structure of an gold (Au)–Ag core–shell nanodome array. Kobayashi and co-workers[27] reported a "voltage-step method" to successfully design a multicolor electrochromic device with electrochemically size-controlled Ag nanoparticles.

L. Dai, X. Lu, L. Song, Prof. Y. Huang, B. Liu, Dr. L. Zhang,
Prof. J. Zhang, Prof. T. Chen
Ningbo Institute of Material Technology and Engineering
Key Laboratory of Graphene Technologies and Applications
of Zhejiang Province
Chinese Academy of Sciences
Ningbo 315201, China
E-mail: huangyouju@mpip-mainz.mpg.de; tao.chen@nimte.ac.cn
L. Dai, X. Lu, L. Song, Prof. Y. Huang, B. Liu, Dr. L. Zhang,
Prof. J. Zhang, Prof. T. Chen
University of Chinese Academy of Sciences
19A Yuquan Road, Beijing 100049, China
Prof. Y. Huang, Dr. S. Wu
Max Planck Institute for Polymer Research
Ackermannweg 10, Mainz D-55128, Germany
E-mail: wusi@mpip-mainz.mpg.de

ADVANCED
SCIENCE NEWS
www.advancedsciencenews.com

ADVANCED
MATERIALS
INTERFACES
www.advmatinterfaces.de

However, due to the complicated control of the morphology and components in these reports, the flexible and cost-effective color display is still hard to be achieved.

Recent works[28] have revealed that polarization can be an easy and powerful approach for modulating the optical response of light in nanomaterials. By controlling the polarization angle, different plasmon modes of nanomaterials can be excited and active polarized colors can be achieved. For instance, our previous work[29] reported that a single Au NR can scatter different colors under the dark-field microscope by taking advantage of the polarized excitation. Similar results about the polarization-dependent anisotropic optical properties of a single Au NR were reported by Link and co-workers[30] and Vaia and co-workers.[31] The ability to scatter multiple colors makes Au NRs as one of the most interesting building blocks for designing SCNMs. Here, we functionalized the original cetyltrimethylammonium bromide (CTAB)-capped Au NRs with methoxypoly(ethylene glycol)thiol (mPEG-SH) via the ligand exchange process and then homogenously dispersed the mPEG-capped Au NRs into the polyvinyl alcohol (PVA) matrix to fabricate the Au NRs/PVA hybrid film. By using a well-developed stretched-film method,[32] mPEG-capped Au NRs embedded in the hybrid film were driven into an oriented alignment along the stretch direction, making the film become polarization-dependent optical response. Systematic study indicated that the stretched hybrid film can macroscopically represent and constructively amplify the anisotropic optical properties of a single Au NR under the polarized excitation. More significantly, the optical color of the stretched hybrid film was finely tuned in a range from green to red under different polarized excitation directions by simply rotating the polarizer. The tunable colors including red, yellow, and green make the Au NRs/PVA hybrid film become a promising candidate for the construction of optical devices.

2. Results and Discussion

2.1. Fabrication and Characterization of Au NRs/PVA Hybrid Films

Au NRs, with an average diameter of 30 ± 1.98 nm and an average length of 110 ± 4.77 nm (**Figure 1**A), were synthesized according to a classical seed-mediated method.[33–35] The aspect ratio distribution of Au NRs was determined from transmission electron microscope (TEM) analysis. As shown in Figure 1B, the nanorods exhibit a relatively narrow aspect ratio distribution. The representative UV-vis-near-infrared (NIR) extinction spectrum in Figure 1C exhibits two clear peaks around 520 and 850 nm corresponding to the SPR of transverse modes and longitudinal modes, respectively.
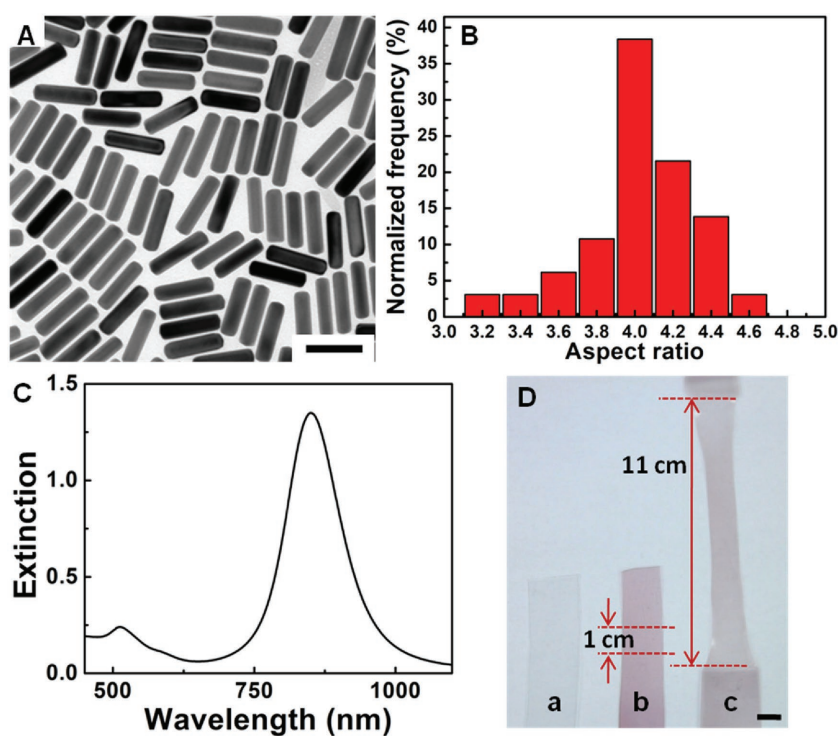

Figure 1. The representative TEM image A) of gold nanorods and B) the corresponding histogram of the nanorod aspect ratio distribution as determined from TEM analysis. The scale bar represents 100 nm. C) The UV–vis–NIR extinction spectrum of Au NRs dispersed in aqueous solution. D) The photographs of polymer films: (a) the pure PVA film, (b) the unstretched hybrid film, and (c) the hybrid film stretched to 11 times of its original length (1 cm), and the scale bar represents 1 cm.

Figure 2A schematically illustrates an effective approach for the fabrication of the nanoparticle/polymer hybrid films, involving the transfer of presynthesized Au NRs into the PVA matrix. In this case, the dispersion and orientation of Au NRs within the PVA matrix are intensively considered because both parameters highly influence the optical properties of the hybrid film. However, in the traditional methods,[3,36,37] for the fabrication of Au nanocrystals (NCs)/PVA nanocomposites, CTAB-capped Au NCs were directly embedded into the PVA matrix. The direct dispersion of the CTAB-capped Au NCs into the PVA films led to the rapid aggregation because of the poor compatibility between CTAB and PVA. Figure 2B clearly shows that the CTAB-capped Au NRs aggregated once they were mixed into the PVA matrix. To avoid this aggregation, the CTAB-capped Au NRs were functionalized with the thio-terminated mPEG-SH. The ligand exchange process is shown in Figure 2A (1) that the CTAB can be easily replaced with the mPEG-SH because of the stronger gold–sulfur bond (40–50 kcal mol^{-1})[38] than the gold–nitrogen bond (8 kcal mol^{-1}).[39,40] The mPEG-SH plays two decisive factors differing from the CTAB. First, due to the strong hydrogen bond interaction and good compatibility between mPEG and PVA,[41–43] mPEG-capped Au NRs can be homogenously dispersed into the PVA matrix without aggregation. The photograph in Figure 1D-a shows that the pure PVA film without Au NRs is colorless and transparent. Interestingly, the hybrid film containing PEG-capped Au NRs appears uniformly red (Figure 1D-b), which suggests the good dispersion of Au
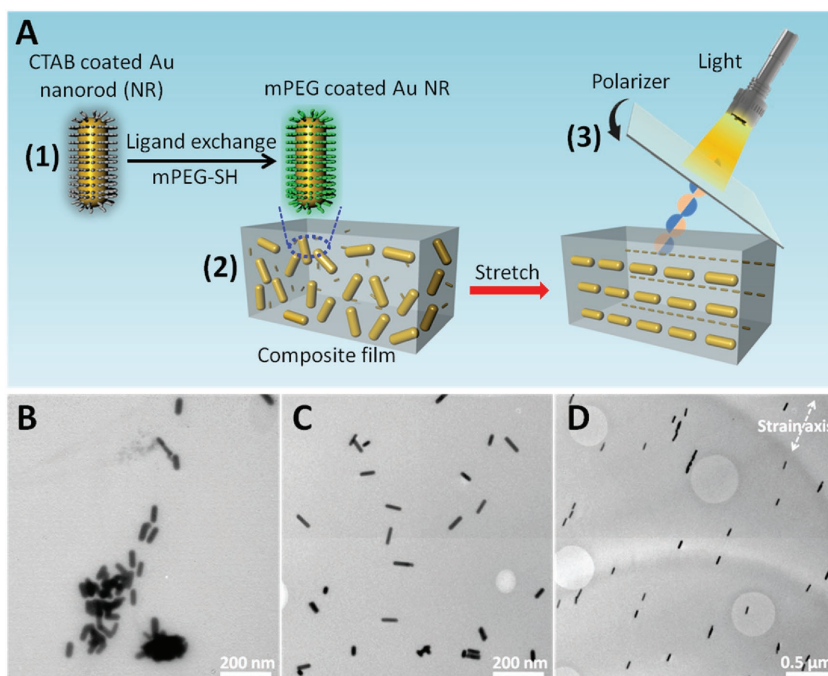
**ADVANCED
SCIENCE NEWS**

www.advancedsciencenews.com

**ADVANCED
MATERIALS
INTERFACES**

www.advmatinterfaces.de

Figure 2. Schematic representation of (A1) the ligand exchange process of Au NRs, (A2) the film-stretched method, and (A3) the polarized excitation process. Representative TEM images of the hybrid films containing Au NRs capped with different ligands: B) CTAB-capped Au NRs and C) mPEG-capped Au NRs before stretch. The TEM image D) of the hybrid film containing mPEG-capped Au NRs after stretch and the length of the stretched film is 11 times of its original length (1 cm). The white-dashed line indicates the direction of the stretch.

NRs in the hybrid films. More intuitive distribution of Au NRs can be observed in the TEM image (Figure 2C), mPEG-capped Au NRs are homogeneously dispersed in the PVA matrix without aggregation as compared to the CTAB-capped Au NRs (Figure 2B). Additionally, because of the good dispersion, higher particle density ($\approx 12.4 \times 10^{-9}$ M, shown in Figure S1 in the Supporting Information) can be obtained to enhance the optical properties of the hybrid film, as compared to previous reports.[44] Second, the strong intermolecular interaction can drive Au NRs to align along the elongation direction of PVA molecule chains during the stretch process, which to some extent ensures a macroscopic and oriented alignment of Au NRs.

The alignment of Au NRs in a preferred direction within the PVA matrix was achieved by utilizing a well-developed stretched-film method schematically shown in Figure 2A (2). Before the stretch, as shown in Figure 2C, the Au NRs were randomly dispersed in the polymer matrix. Subsequently, the hybrid film was cut into a rectangular shape and mechanically stretched along one directon until a desired length was achieved. In our case, the maximal length of the stretched film was chosen to be 11 times of its original length (1 cm), which ensured the almost complete alignment of AuNRs within the stretched film.[45] During the stretch process, the PVA molecular chains elongate along the stretch direction under strain, which drives the longitudinal axes of Au NRs to oriente along the stretch direction.[32,46] The streched hybrid film presented in Figure 1D-c shows good stretchability and uniformity. Figure 2D shows the TEM image of the stretched film, suggesting that the Au NRs became ordered and formed into an oriented alignment along

the stretch direction. Additionally, another two samples, before and after stretch, were measured and the TEM images (Figure S2, Supporting Information) show the same experimental results as Figure 2C,D, indicating the good repeatability.

2.2. Optical Properties of Au NRs/PVA Hybrid Films

Figure 3 shows the UV–vis–NIR extinction spectra of the unstretched and stretched Au NRs/PVA hybrid films under the polarized light at various intermediate polarization angles. Prior to stretch, the film exhibits two clear plasmon peaks arising from the transversal and longitudinal SPR modes of Au NRs shown in Figure 3A. But the intensity of the two plasmon peaks is irrespective of the polarized light directions. As shown in Figure 3D-a,b, the intensity of both plasmon mode peaks has no changes as the polarization angle varies from 0° to 360°, which can be attributed to the random dispersion of Au NRs within the hybrid film. Since though the incident light was polarized in one direction, the collective SPR excited from the randomly dispersed Au NRs was averagely the same. Interestingly, when the film was stretched to 1.5 times of its original length (1 cm) and then measured under the polarized light with different incident angles, the intensity of both plasmon peaks had a slight change shown in Figure 3B. Because the Au NRs began to be driven into an oriented alignment along the stretch direction during the stretch process. However, the change in the intensity was relatively weak due to the low degree of order of the Au NRs. In order to improve the degree of order and ensure that almost all of Au NRs were oriented, the hybrid film was stretched to the maximum length (11 times of its original length (1 cm)). In this case, obvious changes in the intensity are observed when the polarization angle changes from 0° to 90° shown in Figure 3C. Notably, it can be clearly found that either of two plasmon peaks will nearly disappear as long as the other one reaches its maximum. It is easy to understand that the longitudinal plasmon mode is selectively excited when the spectrum is measured under light polarized parallel (0°) to the stretch direction of the film, whereas only the transverse plasma mode is excited under light polarized perpendicular (90°) to the stretch direction. This unique relationship in Figure 3D-c,d further suggests that Au NRs within the PVA film have a good alignment along the stretch direction, which is consistent with the TEM results (Figure 2D and Figure S2B, Supporting Information). Additionally, Figure 3D-c,d shows the intensity of the plasmon peaks undergoes a periodic change as the polarization angle changes from 0 to 360°, indicating that the plasmonic optical response was periodic.

After the stretch, the optical response of the hybrid film becomes polarization dependent. Figure 2A (3) clearly shows
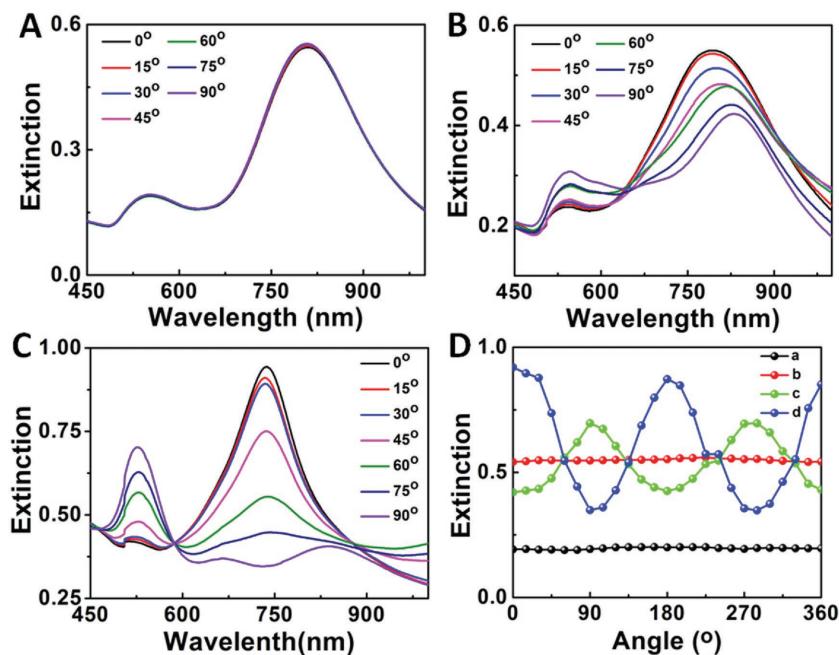
**ADVANCED
SCIENCE NEWS**
www.advancedsciencenews.com

**ADVANCED
MATERIALS
INTERFACES**
www.advmatinterfaces.de

Figure 3. UV–vis–NIR extinction spectrum of A) the unstretched Au NRs/PVA hybrid film, hybrid films stretched 1.5 times for panel (B), and 11 times for panel (C) with different excitation angles of the polarized light. The variation of the intensity of the absorbance with changes of the angle at D) different wavelength: Transverse mode (a) and longitudinal mode (b) peaks of the unstretched hybrid film. Transverse mode (c) and longitudinal mode (d) peaks of the stretched hybrid film (11 times).

the polarized excitation process: First, the original light is polarized after passing through a polarizer and then shines on the streched hybrid film. Due to the oriented alignment, all Au NRs within the film are selectively excited under the same polarization angle, making the hybrid film display the same collective plasmonic color. In such a way, the hybrid film can macroscopically show the anisotropic optical properties of one single Au NR. Besides, As disscused in Figure 3, the excitation mode of the Au NRs can be varied between the transversal and longitudinal plasmon resonance modes by changing the polarization

angle, leading to the ability of hybrid film to display different plasmonic colors. **Figure 4** shows that the hybrid film exhibits a variety of colors including green, yellow, orange, and red at various polarization angles. Besides, we randomly recorded the color of the different regions in the same sample. As shown in Figure S3 (Supporting Information), Regions 1, 2, and 3 almost show the same color under the same excitation angle, which suggests the color is uniform in one sample. This can be attributed to the uniform dispersion of Au NRs within the film. Meanwhile, the optical property of the film is very stable with time. Both Figure 4 and Figure S3 (Supporting Information) (Figure S3 was taken more than 1 month later than Figure 4 from the same sample) show the similar color. More importantly, the color transform goes through a cycle change from green to red to green, which is consistent with the intensity variation of the plasmon peak (shown in Figure 3D-c,d). This indicated that the color of Au NRs/PVA hybrid film can be smartly adjusted by simply rotating the polarizer. In addition, the color variation is continuous and some transitional colors such as yellow and orange can be obtained (shown in Figure 4B,C), which largely ensures the integrity of the color. As a control group, the light spot of the pure PVA film exhibits white color under the polarized light (Figure 4H), which strongly suggests that the gorgeous color is produced by the Au NRs within the hybrid film.

2.3. Potential Application of Au NRs/PVA Hybrid Films

Due to the multicolor displays property, we conceptually present an idea of applying the hybrid film in the field of optical
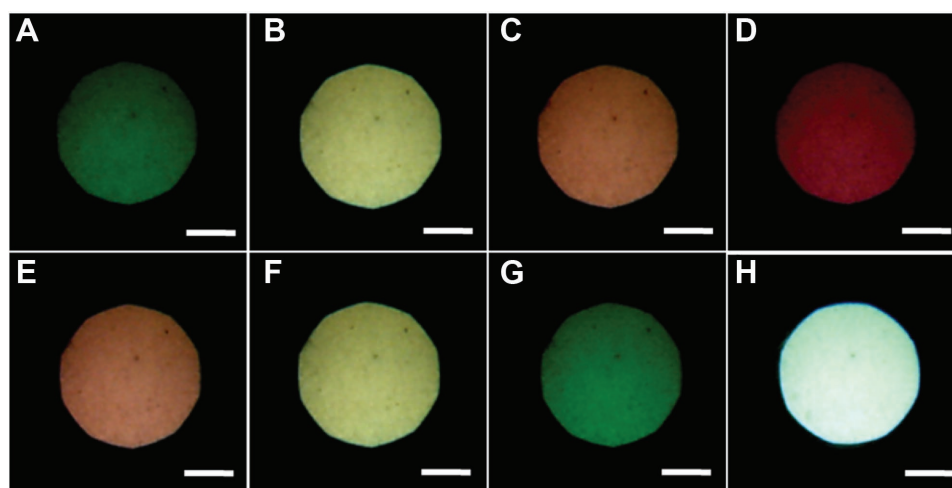

Figure 4. Optical microscopy images of the stretched Au NRs/PVA hybrid film (11 times of its original length (1 cm)) under A–G) the polarized light illumination with different angles: 0, 30, 60, 90, 120, 150, and 180°, and H) the image of the blank sample. The scale bar represents 20 μm.
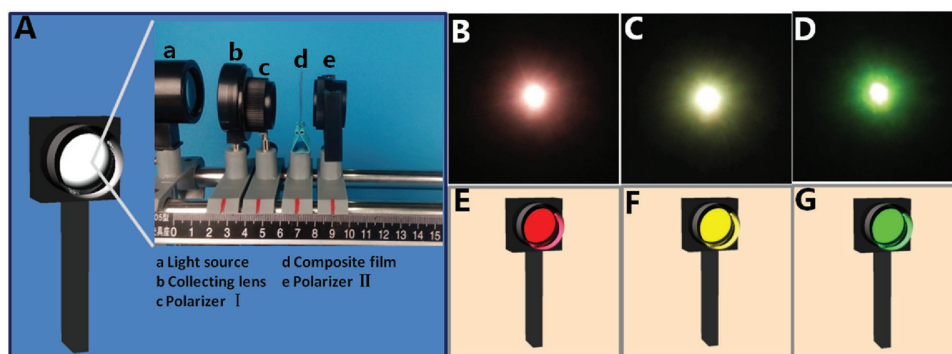
Figure 5. A) The photograph of the homemade traffic light device. B–D) The different colors of the lamp with different polarized light angles: 90, 30, and 0°, and E–G) the schematic representation of the corresponding traffic light modes.

devices such as homemade traffic light devices. **Figure 5**A shows a set of luminous device where the hybrid film (d) can be selectively excited by rotating the polarizer (c). Moreover, the collecting lens (b) play a crucial role: keeping a suitable distance with the light source to obtain a beam of parallel light source. As shown in Figure 5B–D, the luminous device can emit red, yellow, and green light by rotating the polarizer (c). In order to make the color more clear, the polarizer (e) is added to remove undesired excitation colors. A homemade traffic light, based on the Au NRs/PVA hybrid film, is successfully produced by placing the luminous device in a traffic light model (shown in Figure 5E–G). Although this is a conceptual idea, the hybrid film with multicolor displays would be promising in some practical color displays and smart optical devices.

3. Conclusion

We have demonstrated a simple, robust strategy to fabricate a polarization-dependent Au NRs/PVA hybrid film by homogeneously embedding the mPEG-capped Au NRs into the PVA matrix and then drove the Au NRs to form into an oriented alignment along the stretch direction via a well-developed film-stretched method. Under the polarized excitation, the stretched hybrid film can macroscopically represent and constructively amplify the anisotropic optical properties of one single Au NR. Importantly, the optical color can be finely tuned in a range from red to green by simply changing the polarization angle, and the ability to scattering multicolors makes the hybrid film become a promising candidate for the construction of smart optical devices and color displays.

4. Experimental Section

Materials: Tetrachloroauric acid (HAuCl$_4$·4H$_2$O, 99%) and mPEG-SH (MW 2000, 95%) were purchased from J&K Chemicals. CTAB (99%) was purchased from Sigma-Aldrich. Sodium borohydride (NaBH$_4$, 96%), hydrogen chloride (HCl, 36%–38%), and L-ascorbic acid (AA) (C$_6$H$_8$O$_6$, 99.7%) were purchased from Sinopharm Chemical Reagent Co., Ltd. Silver nitrate (AgNO$_3$, 99%) was purchased from Aladdin Industrial Corporation in Shanghai. Sodium oleate (NaOL) was supplied by TCI (Shanghai) Development Co., Ltd. Polyvinyl alcohol 124 GR (viscosity:

54.0–66.0 mPa·s, alcoholysis: 98.0–99.8 mol %) was purchased from Vokai Chemical Reagent Co., Ltd.

Instruments: UV–vis–NIR extinction spectra were recorded by Lambda 950 UV–vis–NIR spectrophotometer from Perkin-Elmer Instrument Co. Ltd US and the structures of gold nanorods were observed by transmission electron microscopy, which was conducted on the JEOL JEM2010 electron microscope. Hybrid films with different draw ratio were obtained by using the universal test tensile machine (Instron5567). The optical properties of hybrid films were recorded by the polarized light microscope (BX51-P, OLYMPUS).

Synthesis of Gold Nanorods: In order to synthesize uniform Au NRs, the seed solution for Au NRs growth was prepared as follows: 0.1 mL of 25 × 10^{-3} M HAuCl$_4$ was dissolved in 4.9 mL deionized water and then was mixed with 5 mL of 0.2 M CTAB in a 20 mL glass bottle. Subsequently, 100 mL of fresh 0.006 M NaBH$_4$ was prepared and rapidly 1 mL of the NaBH$_4$ solution was injected to the HAuCl$_4$-CTAB solution under vigorous stirring (1200 rpm). The stirring was stopped after 2 min and the seed solution color changed from yellow to brownish yellow. Finally, the solution was placed without disturbance at room temperature for 30 min before use.

The Au NRs growth solution was prepared as follows: 2.8 g (0.077 M) of CTAB and 0.4936 g (0.016 M) of NaOL were dissolved in 100 mL of warm (50 °C) deionized water. The mixed solution was cooled down to 30 °C and 7.2 mL AgNO$_3$ solution (1.0 × 10^{-3} M) was added. The mixture was placed without undisturbed at 30 °C for 15 min and then 100 mL of HAuCl$_4$ (1.0 × 10^{-3} M) solution was added under magnetic stirring (700 rpm). The solution became colorless after 90 min and 0.6 mL of HCl solution (37 wt % in water, 12.1 M) was added under magnetic stirring (400 rpm) for 15 min. Then, 0.5 mL of AA solution was added and the solution was vigorously stirred (1200 rpm) for 30 s after which 160 µL of seed solution was injected into the growth solution with another stir (1200 rpm) for 30 s. In the end, the solution was left undisturbed at 30 °C for 12 h for Au NRs growth. The obtained Au NRs were characterized by UV–vis–NIR spectrum and transmission electron microscope (shown in Figure 1A,C).

Preparation of mPEG-Capped Au NRs: The original CTAB-capped Au NRs were functionalized with the mPEG-SH according to a reported method.[47] In a typical process, 200 mL original CTAB-capped Au NRs solution was centrifuged at 8000 rpm for 10 min to remove the excess CTAB. After the centrifugation, the supernatant was removed and the precipitate was renewably dispersed in 20 mL deionized water. The purification process was carried out two times. 2 mL of 10 × 10^{-3} M mPEG-SH was added into the 20 mL Au NRs solution and then the mixture was placed with slight stir under room temperature for 12 h. The excess mPEG-SH was removed by centrifugation at 7000 rpm for 10 min and the Au NRs precipitate was washed once with water by the centrifugation at the same condition and then redispersed in 1 mL deionized water for further use.

Fabrication of Au NRs/PVA Hybrid Films: 13 g PVA was dissolved in 97 mL deionized water under oil bath (95 °C) for a while until PVA was

**ADVANCED
SCIENCE NEWS**

www.advancedsciencenews.com

**ADVANCED
MATERIALS
INTERFACES**

www.advmatinterfaces.de

completely dissolved. Then 10 mL PVA aqueous solution and 1 mL mPEG-capped Au NRs solution were mixed under vigorous stirring (1000 rpm). The uniform mixed solution was poured into a glass ware under room temperature for several days. The Au NRs/PVA hybrid film was obtained after the water evaporated. The hybrid films with different draw ratio were achieved under the strain (the strain rate: 20 mm min^{-1}) by using the universal test tensile machine (Instron5567).

Preparation of TEM Samples of Au NRs/PVA Hybrid Films: TEM samples of Au NRs/PVA hybrid films were prepared by embedding the stripes of the Au NRs/PVA hybrid films into an epoxy resin. Briefly, the appropriate ratio of the epoxy resin was obtained by uniformly mixing 4 g 3,4-epoxycyclohexylmethyl 3,4-epoxycyclohexanecarboxylate (ERL-4221), 1.5 g Dow 736 epoxy resin (DER-736), 6.5 g nonenylsuccinic anhydride, and 0.1 g *N*,*N*-dimethylethanolamine. Subsequently, the stripes of thin hybrid films were embedded into the mixture and then placed in the drying oven at 75 °C for 8 h. The solidified stripes were sliced in an ultramicrotome (RMC1) with a glass knife to a thickness of 70 nm and deposited on a copper grid. The ultramicrotomed samples were imaged in a JEOL JEM2100 TEM.

Supporting Information

Supporting Information is available from the Wiley Online Library or from the author.

Acknowledgements

Conflict of Interest

The authors declare no conflict of interest.

Keywords

[1] Y. Zhao, Z. Xie, H. Gu, C. Zhu, Z. Gu, *Chem. Soc. Rev.* **2012**, *41*, 3297.

[2] G. Wang, X. Chen, S. Liu, C. Wong, S. Chu, *ACS Nano* **2016**, *10*, 1788.

[3] P. Zijlstra, J. W. Chon, M. Gu, *Nature* **2009**, *459*, 410.

[4] S. N. Varanakkottu, M. Anyfantakis, M. Morel, S. Rudiuk, D. Baigl, *Nano Lett.* **2016**, *16*, 644.

[5] S. Kawata, Y. Kawata, *Chem. Rev.* **2000**, *100*, 1777.

[6] J. W. M. Chon, C. Bullen, P. Zijlstra, M. Gu, *Adv. Funct. Mater.* **2007**, *17*, 875.

[7] T. Xu, Y. K. Wu, X. Luo, L. J. Guo, *Nat. Commun.* **2010**, *1*, 59.

[8] S. M. Lee, D. Kim, D. Y. Jeon, K. C. Choi, *Small* **2012**, *8*, 1350.

[9] Z. Feng, C. Jiang, Y. He, S. Chu, G. Chu, R. Peng, D. Li, *Adv. Opt. Mater.* **2014**, *2*, 1174.

[10] L. Zhu, W. L. Ong, X. Lu, K. Zeng, H. J. Fan, G. W. Ho, *Small* **2017**, *13*, 1700084.

[11] L. Guo, Y. Xu, A. R. Ferhan, G. Chen, D. H. Kim, *J. Am. Chem. Soc.* **2013**, *135*, 12338.

[12] J. Du, L. Jiang, Q. Shao, X. Liu, R. S. Marks, J. Ma, X. Chen, *Small* **2013**, *9*, 1467.

[13] S. Y. Choi, M. Mamak, G. von Freymann, N. Chopra, G. A. Ozin, *Nano Lett.* **2006**, *6*, 2456.

[14] X. Hong, Y. Peng, J. Bai, B. Ning, Y. Liu, Z. Zhou, Z. Gao, *Small* **2014**, *10*, 1308.

[15] P. Joo, K. Jo, G. Ahn, D. Voiry, H. Y. Jeong, S. Ryu, M. Chhowalla, B.-S. Kim, *Nano Lett.* **2014**, *14*, 6456.

[16] K. Iwasaki, T. Torimoto, T. Shibayama, T. Nishikawa, B. Ohtani, *Small* **2006**, *2*, 854.

[17] J. Seidel, W. Luo, S. J. Suresha, P. K. Nguyen, A. S. Lee, S. Y. Kim, C. H. Yang, S. J. Pennycook, S. T. Pantelides, J. F. Scott, R. Ramesh, *Nat. Commun.* **2012**, *3*, 799.

[18] A. Peters, N. R. Branda, *J. Am. Chem. Soc.* **2003**, *125*, 3404.

[19] H. S. Lee, T. S. Shim, H. Hwang, S.-M. Yang, S.-H. Kim, *Chem. Mater.* **2013**, *25*, 2684.

[20] T. Du, J. Schneider, A. K. Srivastava, A. S. Susha, V. G. Chigrinov, H. S. Kwok, A. L. Rogach, *ACS Nano* **2015**, *9*, 11049.

[21] H. P. Deng, Y. Su, M. X. Hu, X. Jin, L. He, Y. Pang, R. J. Dong, X. Y. Zhu, *Macromolecules* **2015**, *48*, 5969.

[22] S. I. Bozhevolnyi, V. S. Volkov, E. Devaux, J.-Y. Laluet, T. W. Ebbesen, *Nature* **2006**, *440*, 508.

[23] J. Z. Zhang, *Acc. Chem. Res.* **1997**, *30*, 423.

[24] S. K. Ghosh, T. Pal, *Chem. Rev.* **2007**, *107*, 4797.

[25] Y. Jin, N. Friedman, *J. Am. Chem. Soc.* **2005**, *127*, 11902.

[26] L. Shao, X. Zhuo, J. Wang, *Adv. Mater.* **2018**, *30*, 1704338.

[27] A. Tsuboi, K. Nakamura, N. Kobayashi, *Adv. Mater.* **2013**, *25*, 3197.

[28] Z. Li, A. W. Clark, J. M. Cooper, *ACS Nano* **2016**, *10*, 492.

[29] Y. Huang, D. H. Kim, *Nanoscale* **2011**, *3*, 3228.

[30] W. S. Chang, J. W. Ha, L. S. Slaughter, S. Link, *Proc. Natl. Acad. Sci. USA* **2010**, *107*, 2781.

[31] S. Biswas, D. Nepal, K. Park, R. A. Vaia, *J. Phys. Chem. Lett.* **2012**, *3*, 2568.

[32] D. Fornasiero, F. Grieser, *Chem. Phys. Lett.* **1987**, *139*, 103.

[33] Y. Huang, L. Wu, X. Chen, P. Bai, D.-H. Kim, *Chem. Mater.* **2013**, *25*, 2470.

[34] X. Ye, C. Zheng, J. Chen, Y. Gao, C. B. Murray, *Nano Lett.* **2013**, *13*, 765.

[35] C. L. Zhang, K. P. Lv, H. P. Cong, S. H. Yu, *Small* **2012**, *8*, 647.

[36] C. J. Murphy, C. J. Orendorff, *Adv. Mater.* **2005**, *17*, 2173.

[37] K. Choi, P. Zijlstra, J. W. M. Chon, M. Gu, *Adv. Funct. Mater.* **2008**, *18*, 2237.

[38] H. Hinterwirth, S. Kappel, T. Waitz, T. Prohaska, W. Lindner, M. Lammerhofer, *ACS Nano* **2013**, *7*, 1129.

[39] K. Liu, Y. Zheng, X. Lu, T. Thai, N. A. Lee, U. Bach, J. J. Gooding, *Langmuir* **2015**, *31*, 4973.

[40] T. M.-P. Gschneidtner, *Handbook of Single Molecule Electronics*, Pan Stanford Publishing Pte Ltd., Singapore **2009**, p. 23.

[41] L. Masaro, X. X. Zhu, *Langmuir* **1999**, *15*, 8356.

[42] Y. Li, W. Wu, F. Lin, A. Xiang, *J. Appl. Polym. Sci.* **2012**, *126*, 162.

[43] L. Masaro, X. X. Zhu, P. M. Macdonald, *Macromolecules* **1998**, *31*, 3880.

[44] C. Fang, L. Shao, Y. Zhao, J. Wang, H. Wu, *Adv. Mater.* **2012**, *24*, 94.

[45] B. M. I. van der Zande, L. Pagès, R. A. M. Hikmet, A. van Blaaderen, *J. Phys. Chem. B* **1999**, *103*, 5761.

[46] J. Michl, E. W. Thulstrup, J. H. Eggers, *J. Phys. Chem.* **1970**, *74*, 3878.

[47] M. Xiao, H. Chen, T. Ming, L. Shao, J. Wang, *ACS Nano* **2010**, *4*, 6565.